Electrons in a Periodic Magnetic Field Induced by a Regular Array of Micromagnets

P. D. Ye,[1] D. Weiss,[1] R. R. Gerhardts,[1] M. Seeger,[2] K. von Klitzing,[1] K. Eberl,[1] and H. Nickel[3]

[1]*Max-Planck-Institut für Festkörperforschung, D-70569 Stuttgart, Germany*

[2]*Max-Planck-Institut für Metallforschung, Institut für Physik, D-70569 Stuttgart, Germany*

[3]*Forschungsinstitut der Deutschen Bundespost, D-64295 Darmstadt, Germany*

(Received 2 December 1994)

The deposition of ferromagnetic microstructures on top of a high-mobility two-dimensional electron gas (2DEG) allows the investigation of electron transport in a *periodic magnetic field* which alternates on a length scale small compared to the elastic mean free path of the electrons. The longitudinal resistance of the 2DEG displays, as a function of the externally applied field, the long-predicted *magnetic* commensurability oscillations which result from the interplay between the two characteristic length scales of the system, the classical cyclotron radius R_c of the electrons and the period a of the magnetic field modulation.

PACS numbers: 73.50.Jt, 73.20.Dx, 75.50.Rr

Transport properties of electrons in a two-dimensional electron gas (2DEG) subjected to a periodic *magnetic* field have attracted considerable theoretical interest [1–6]. Depending on the strength of the local magnetic field, the electron motion in the plane of the 2DEG can be tuned from regular to chaotic. The motion of ballistic *electrons* in a periodic magnetic field is also believed to be closely related to the motion of *composite fermions* in a density modulated 2DEG in the fractional quantum Hall regime [7]. Distinct theoretical predictions exist for the limit of a weak one-dimensional (1D) magnetic modulation (modulation amplitude $|B_m| \ll |B_0|$, the external magnetic field) where the magnetoresistance ρ_{xx} is expected to oscillate with minima appearing at magnetic fields given by [2–5]

$$2R_c = \frac{2\hbar k_F}{e|B_0|} = \left(\lambda + \frac{1}{4}\right)a, \tag{1}$$

where $\lambda = 0, 1, \ldots$ is an integer oscillation index, $k_F = \sqrt{2\pi n_s}$ the Fermi wave number, with n_s the carrier density of the 2DEG, and a the period of the 1D modulation in the x direction. This predicted effect is closely related to the commensurability oscillations observed recently in the resistivity ρ_{xx} of a 2DEG with weak electric modulation [8–10]. Similar to the electric case, the magnetic modulation leads to a modified energy spectrum [1–5]. The degenerate Landau levels are transformed into bands of finite width. The dispersion of these Landau bands provides an additional contribution to the resistivity ρ_{xx}, which vanishes only when the bandwidth becomes zero ("flat-band condition") [9,10]. In contrast to Eq. (1), which is the flat-band condition for magnetic modulation, the flat-band condition for weak electrical modulation reads $2R_c = (\lambda - 1/4)a$ with $\lambda = 1, 2, \ldots$. Hence, ρ_{xx} of a 2DEG with a weak electric modulation displays minima at B_0 fields where in a weak magnetic modulation of the same period a maxima are expected.

For the case of a pure electric modulation, the additional contribution to ρ_{xx} has been related to the classical guiding center drift of the cyclotron orbits which vanishes if the flat-band condition holds [11]. This classical picture is easily extended to include in addition to a modulation $V_m(x) = V_m \cos Kx$ of the electrostatic potential energy of an electron a weak modulation $B_m(x) = B_m \cos Kx$ of the z component of the magnetic field ($K = 2\pi/a$). Averaging the modulation induced drift of the guiding centers over the unperturbed cyclotron orbits at field B_0 [11,12], we obtain for the resulting change in the resistivity

$$\frac{\Delta\rho_{xx}}{\rho_0} = \frac{2\tau^2}{\pi\hbar^2 n_s a R_c}|S|^2, \tag{2}$$

where ρ_0 is the zero-field resistivity of the unmodulated 2DEG, τ is the scattering time, and

$$S = V_m \cos\left[KR_c - \frac{\pi}{4}\right] \pm \frac{k_F a}{2\pi}\hbar\omega_m \sin\left[KR_c - \frac{\pi}{4}\right], \tag{3}$$

with $\omega_m = eB_m/m^*$ (m^* is the effective electron mass of GaAs). The "+" in Eq. (3) holds if $B_0 > 0$, and the "−" sign holds if the applied field (and thus the direction of the cyclotron motion) is reversed, $B_0 < 0$, while $V_m(x)$ and $B_m(x)$ are fixed [13]. The zeros of Eq. (3) and hence the flat-band positions now depend on the relative strengths of electric and magnetic modulations, V_m and $\hbar\omega_m$, respectively.

Over the last years a variety of experimental attempts were made (e.g., [5]) to establish a periodic magnetic field on the length scale of a few hundred nanometer, so far, however, without success. In this Letter we report a novel method to investigate electron transport in a *periodic magnetic* field. By depositing an array of ferromagnetic dysprosium (Dy) strips with widths of a few hundred nanometer on top of a semiconductor heterojunction (Fig. 1), we generate a 1D periodic magnetic field in the plane of the 2DEG. By increasing the strength of these micromagnets via the externally applied field we show that the long-desired *magnetic* commensurability oscillations appear in the resistivity ρ_{xx}.

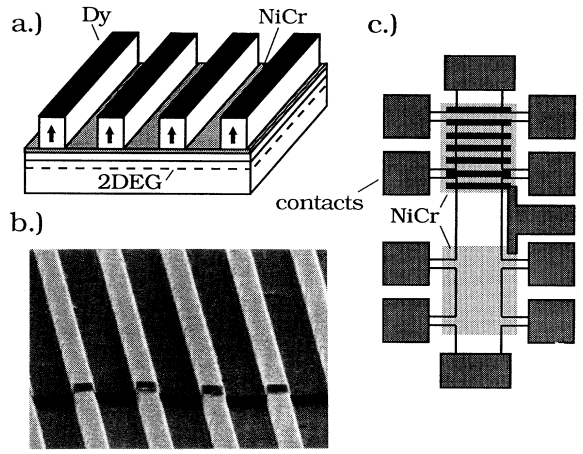

FIG. 1. (a) Sketch of the one-dimensional ferromagnetic Dy grating on top of a GaAs-AlGaAs heterojunction. (b) Electron micrograph of the Dy strips evaporated across a mesa edge: $a = 1\ \mu$m, height of a Dy strip: 200 nm. (c) Device geometry containing the ferromagnetic grating and an unpatterned reference Hall bar.

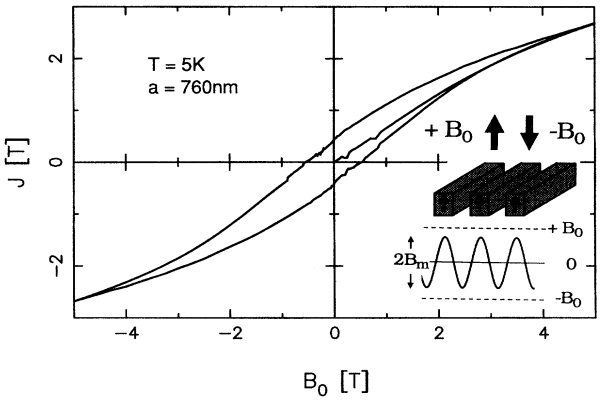

FIG. 2. Hysteresis of the magnetic polarization J measured from a large array (5×5 mm^2) of Dy wires prepared by holographic lithography on a GaAs substrate. The inset sketches the normal component $B_m(x)$ of the stray field induced by the micromagnets in the plane of the 2DEG. Reversing the external magnetic field results in a phase shift of the modulation with respect to the grating (see text).

Our samples were prepared from high-mobility GaAs-AlGaAs heterojunctions where the 2DEG was located approximately 100 nm underneath the sample surface. The carrier density n_s and electron mobility μ at 4.2 K were $\sim 2.2 \times 10^{11}$ cm^{-2} and 1.3×10^6 cm^2/V s, respectively, corresponding to an elastic mean free path of $\sim 10\ \mu$m. 50 μm wide Hall bars, sketched in Fig. 1(c), were fabricated by standard photolithographic techniques. Alloyed AuGe/Ni pads contact the 2DEG. A 10 nm thin NiCr film, evaporated on top of the devices, defines an equipotential plane to avoid electric modulation of the 2DEG. However, strain due to different thermal expansion coefficients of the ferromagnetic grating and the heterojunction always results in a weak electric periodic potential as the sample is cooled down to cryogenic temperatures (see below). The Dy gratings with period of 500 nm and 1 μm were defined by electron beam lithography on top of one of the NiCr gates. After developing the exposed PMMA resist a 200 nm Dy film was evaporated. After lift-off in acetone micromagnet arrays, like the one shown in Fig. 1(b), were obtained. For magnetization measurements, large area (5×5 mm^2) Dy wire arrays with comparable wire width were prepared by holographic lithography. Four point resistance measurements were performed in a ^{4}He cryostat with superconducting coils using standard ac lock-in techniques. For all experiments, the external magnetic field B_0 was applied normal (z direction) to the plane of the 2DEG.

Measurements of the macroscopic stray fields of the large array of holographically prepared Dy wires ($a =$ 760 nm) were measured with a Quantum Design SQUID magnetometer. The resulting hysteresis loop shown in Fig. 2 indicates hard magnetic behavior of the Dy wires. The coercive field B_c of 0.5 T is high compared to pure polycrystalline Dy ($B_c < 50$ mT). Hence, the demagnetization process is controlled either by the pinning or the nucleation mechanism [14]. The stray field $B_m(x)$ in the z direction, sketched in the inset of Fig. 2, is expected to alternate with an average value close to zero [4]. We return to this point below.

Figure 3(a) shows the resistivity ρ_{xx} of the 2DEG underneath the Dy superlattice with period $a = 1\ \mu$m. Since the devices with $a = 500$ nm display comparable behavior, we concentrate on the larger period sample below. The traces labeled 1–10 T are obtained as follows: After the initial cooldown we first sweep to 1 T and measure the ρ_{xx} trace labeled 1 T from 1 to -0.25 T. Then we sweep to $B^{\max} = 2$ T and take the next ρ_{xx} trace in the same B_0 interval. By successively sweeping to higher $B^{\max}$ (up to 10 T) the magnetic polarization J in the Dy strips and hence the strength of the resulting periodic field $B_m(x)$ are increased. This enhanced strength affects the magnetoresistance traces: ρ_{xx} displays oscillations with a dramatically growing maximum between $B_0 = 0.15$ and 0.75 T (the superimposed oscillations above 0.5 T are Shubnikov–de Haas oscillations). For positive B_0, the minima in ρ_{xx} appear at B_0 values expected from Eq. (1) for *magnetic* modulation [15]. From the amplitude $\Delta\rho_{xx}$ of the maxima at $B_0 \sim 0.3$ T we estimate the amplitude of the imposed magnetic field B_m from Eq. (2) with $2R_c \approx 0.75a$. This gives B_m values, plotted in the inset of Fig. 3(a), which range between 13 mT for the $B^{\max} = 1$ T trace and 40 mT for the $B^{\max} = 10$ T trace. At low B_0 the traces are not symmetric with respect to $B_0 = 0$ as is expected for a broken time reversal symmetry [16]. This can be seen clearly in Fig. 3(b) where the low B_0 regime of Fig. 3(a) is magnified. With increasing $B^{\max}$ a richer oscillatory structure unfolds in ρ_{xx} indicating a growing magnetic field modulation. The ρ_{xx} minima for $B_0 > 0$ of trace e almost perfectly coincide

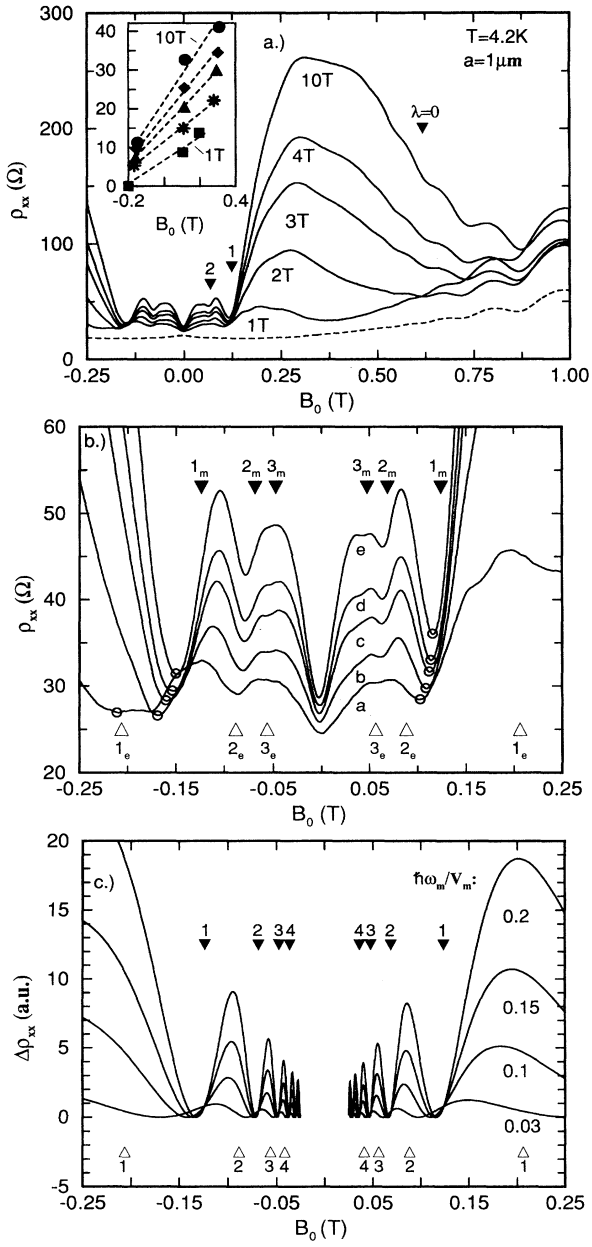

FIG. 3. (a) ρ_{xx} vs external magnetic field B_0 for different $B^{\max}$ sweeps. Filled triangles with positions defined by Eq. (1) mark the flat-band condition in a periodic magnetic field. The inset displays the strength of the magnetic modulation B_m (in mT) as a function of B_0, derived from (i) the amplitude of the large resistance maximum at $\sim$0.3 T and (ii) the positions of the ρ_{xx} minima in (b) around -0.16 and 0.12 T. (b) Low-field magnification of (a) showing the shift of the ρ_{xx} minima with increasing $B^{\max}$ (from $a = 1$ T to $e = 10$ T). Filled triangles mark the position of the *magnetic* flat-band condition (subscript "m") while the open triangles mark the *electric* ones (subscript "e"). The open circles highlight the positions of the ρ_{xx} minima used to evaluate the B_m's from the zeros of Eq. (3). (c) $\Delta\rho_{xx}$ calculated for different $\hbar\omega_m/V_m$ ratios using Eq. (2). Filled and open triangles again mark magnetic and electric flat-band conditions.

with what is expected from Eq. (1), indicating that the periodic magnetic field dominates over the weak electric potential. These are the long predicted *magnetic* commensurability oscillations.

The polarization J (Fig. 2) and hence the stray field $B_m(x)$ of the micromagnets depend (besides on $B^{\max}$) on B_0. Therefore one expects to reduce B_m by sweeping toward the coercive field B_c around -0.5 T [17]. However, following trace a in Fig. 3(b) to negative B_0 one still observes oscillations in ρ_{xx}. But now the minima in ρ_{xx} ($\lambda = 1, 2$) appear at B_0 positions where one expects minima for pure *electric* modulation with period a, marked by open triangles. The origin of this *electric* modulation is strain caused by the different thermal expansion coefficients of Dy and GaAs. This effect, reported previously for other material combinations [5,18,19], results in a modulation of the band edges in GaAs via the deformation potential. Assuming a sinusoidal modulation we estimate from the amplitude of the resistance maximum at $B_0 \sim -0.12$ T (trace a) an amplitude of the (screened) electric potential V_m of ~ 0.3 meV [20]. The presence of the weak electric modulation which is independent of $B^{\max}$ allows one to "calibrate" the strength of the stray field B_m. If $B^{\max}$ and hence B_m are increased successively (traces b–e) all the ρ_{xx} minima shift from the *electric* flat-band condition (open triangles) to the *magnetic* one (full triangles). If both a periodic potential and an oscillating magnetic field act on the electrons, the flat-band case is determined by the zeros of Eq. (3). Since the position of the flat-band condition depends on the ratio $\hbar\omega_m/V_m$, $\hbar\omega_m$ and hence the field B_m of the micromagnets can be estimated from the B_0 position of the ρ_{xx} minima. The result is shown in the inset of Fig. 3(a). To obtain the B_m's we analyzed the position of the minima between 1_e and 1_m (here, the subscripts of the oscillation index λ, e and m, stand for the electric and the magnetic flat-band conditions, respectively) for reversed B_0, and between 2_e and 1_m for positive B_0. The inset also includes the B_m values estimated independently from the ρ_{xx} maxima between 1_m and 0_m. These B_m values increase linearly with B_0, as is expected from the hysteresis trace in Fig. 2 in this magnetic field range.

The peculiar asymmetry for forward and reverse magnetic fields in Fig. 3(b) is also observed for the minima with higher λ's. The origin of this asymmetry is the switching of the "$\pm$" in Eq. (3) if B_0 is reversed. This change of the sign at $B_0 = 0$ can be viewed as a phase jump of π between the electric modulation $V_m(x)$ and the total magnetic field strength $B(x) = |B_0 + B_m(x)|$. This is illustrated in the inset of Fig. 2. Here, we put the z axis in the direction of $B^{\max}$ and take $x = 0$ in the center of a Dy strip, so that $B_m > 0$. While the phase of the electric modulation (with respect to the ferromagnetic grating) is independent of the B_0 direction, the phase of the periodic B field is not: for $B_0 > 0$ the local maxima of the B field are underneath the Dy strips while for $-B_c < B_0 < 0$ the

maxima are between the strips. This allows an *absolute* measurement of the phase of the electric modulation: Since the sign in Eq. (3) is "+" for $B_0 > 0$ while $B_m > 0$, we obtain the correct shift of the minima for $V_m < 0$, i.e., if n_s is higher underneath the strips [21].

In Fig. 3(c) we display model calculations of ρ_{xx} based on Eq. (2). The $\Delta\rho_{xx}$ oscillations calculated for four different $\hbar\omega_m/V_m$ ratios closely resemble the experimental data in Fig. 3(b). As in the experiment the oscillation minima shift with increasing B_m from the electric flat-band condition to the magnetic flat-band condition. For $\hbar\omega_m/V_m = 0.2$, corresponding to $B_m \sim 40$ mT in our experiment, the ρ_{xx} minima are determined by the magnetic flat-band conditions (filled triangles) indicating the dominance of the periodic B_m field. The asymmetry with respect to the shift of the minima (see, e.g., the shift from $1_e \rightarrow 1_m$ for $B_0 < 0$ and from $2_e \rightarrow 1_m$ for $B_0 > 0$ with increasing B_m) is adjusted to the experiment by choosing $V_m < 0$ (see above). For the sake of simplicity we used, in contrast to experiment, a B_0-independent magnetic field modulation B_m to demonstrate the shift of the ρ_{xx} minima.

If the reversed field is increased beyond the coercive field, the polarization of the micromagnets switches and finally follows the externally applied field. On sweeping back where we start from the corresponding $-B^{\max}$ values we obtain, as is expected from the hysteresis loop (Fig. 2), the mirror image (with respect to the $B_0 = 0$ axis) of the experimental traces shown above.

Now we address the zero-field resistance $\rho_{xx}(B_0 = 0)$ and the positive magnetoresistance at $|B_0| < 30$ mT. First we note that the minimum of ρ_{xx} at $B_0 = 0$ in Fig. 3(b) does not shift with increasing $B^{\max}$ (shift less than 3 mT) while, on the other hand, the amplitude B_m becomes as high as 20 mT at $B_0 = 0$ [see inset of Fig. 3(a)]. Such behavior is expected for an alternating stray field $B_m(x)$ with an average value of zero (inset of Fig. 2). This is consistent with the experimental finding that, independent of $B^{\max}$, the Hall resistance measured in the magnetic superlattice is the same as in the reference Hall bar. The positive low-field magnetoresistance might also be related to this alternating $B_m(x)$ field: electron trajectories "wiggling" along a $B_m(x) = 0$ borderline (open orbits; for the electric case see, e.g., [22]) cause an increasing magnetoresistance which saturates once $|B_0| > |B_m|$. For trace e in Fig. 3(b) the positive magnetoresistance saturates around 28 mT comparable to the B_m value of about 20 mT in the inset of Fig. 3(a). Finally, we note that $\rho_{xx}(0)$ increases linearly with $B_m(0)$, as can be extracted from Fig. 3(b) and the inset of Fig. 3(a). Similar behavior is expected for electrons scattering from microinhomogeneities in a magnetic field [23].

In summary, we have observed the long-predicted commensurability oscillations in the presence of a periodic magnetic field. The experimental technique described above opens up the way to experiments in alternating magnetic fields with periods in the nanometer regime. During the preparation of this manuscript we became aware of similar experiments using patterned superconductors on top of a heterojunction [24].

We thank M. Riek and A. Gollhardt for technical support, and W. Dietsche, H. Kronmüller, J. Smet, and M. Tornow for valuable discussions. P. D. Ye acknowledges the Volkswagen Foundation for a fellowship.

[1] D. Yoshioko and Y. Iye, J. Phys. Soc. Jpn. **56**, 448 (1987).
[2] P. Vasilopoulos and F. M. Peeters, Superlattices Microstruct. **7**, 393 (1990).
[3] F. M. Peeters and P. Vasilopoulos, Phys. Rev. B **47**, 1466 (1993).
[4] D. P. Xue and G. Xiao, Phys. Rev. B **45**, 5986 (1992).
[5] R. Yagi and Y. Iye, J. Phys. Soc. Jpn. **62**, 1279 (1993).
[6] X. Wu and S. E. Ulloa, Solid State Commun. **82**, 945 (1992); G. J. O. Schmidt, Phys. Rev. B **47**, 13 007 (1993); R. B. S. Oakeshott and A. MacKinnon, J. Phys. Condens. Matter **5**, 9355 (1993); P. Schmelcher and D. L. Shepelyansky, Phys. Rev. B **49**, 7418 (1994).
[7] W. Kang, H. L. Störmer, L. N. Pfeiffer, K. W. Baldwin, and K. W. West, Phys. Rev. Lett. **71**, 3850 (1993); R. L. Willet, R. R. Ruel, K. W. West, and L. N. Pfeiffer, Phys. Rev. Lett. **71**, 3846 (1993).
[8] D. Weiss, K. von Klitzing, K. Ploog, and G. Weimann, Europhys. Lett. **8**, 179 (1989).
[9] R. R. Gerhardts, D. Weiss, and K. von Klitzing, Phys. Rev. Lett. **62**, 1173 (1989).
[10] R. W. Winkler, J. P. Kotthaus, and K. Ploog, Phys. Rev. Lett. **62**, 1177 (1989).
[11] C. W. J. Beenakker, Phys. Rev. Lett. **62**, 2020 (1989).
[12] R. R. Gerhardts, Phys. Rev. B **45**, 3449 (1992).
[13] For $B_0 > 0$ and intermediate temperatures ($T_c \ll T \ll T_a$ in the notation of Ref. [3]) Eq. (23) of Ref. [3] is equivalent with our Eq. (2). Because of an incorrect formula for the diffusion tensor, the value given by Eq. (16) of Ref. [4] (for $V_m = 0$) is too small by a factor of 2.
[14] H. Kronmüller, K.-D. Durst, and M. Sagawa, J. Magn. Magn. Mater. **74**, 291 (1988).
[15] The flat-band positions were derived using first order perturbation theory involving the cosine approximation of the Bessel functions [11,12]. Deviations are therefore expected for large values of B_0. This especially affects the $\lambda = 0$ position in Fig. 3(a).
[16] To account for inhomogeneities in our devices we averaged over ρ_{xx} traces taken from potential probes of both sides of the Hall bar.
[17] This is strictly valid only for $B^{\max} = 5$ T. We expect B_c values *around* -0.5 T for the other traces.
[18] J. H. Davies and I. A. Larkin, Phys. Rev. B **49**, 4800 (1994).
[19] P. D. Ye et al. (unpublished).
[20] D. Weiss, Phys. Scr. **T35**, 226 (1991).
[21] GaAs is expected to shrink with respect to Dy if cooled down, resulting in minima of $V_m(x)$ under the strips.
[22] P. H. Beton *et al.*, Phys. Rev. B **42**, 9229 (1990).
[23] A. V. Khaetskii, J. Phys. Condens. Matter **3**, 5115 (1991).
[24] A. K. Geim (private communication).

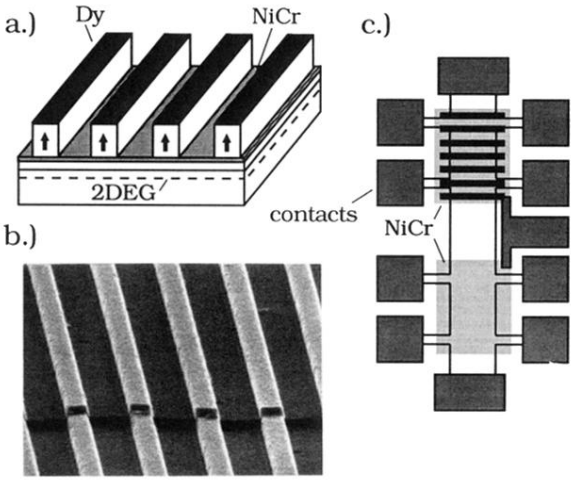

FIG. 1. (a) Sketch of the one-dimensional ferromagnetic Dy grating on top of a GaAs-AlGaAs heterojunction. (b) Electron micrograph of the Dy strips evaporated across a mesa edge: $a = 1\ \mu$m, height of a Dy strip: 200 nm. (c) Device geometry containing the ferromagnetic grating and an unpatterned reference Hall bar.